Synergism between peroxymonosulfate and $LaCoO_3$-TiO_2 photocatalysis for oxidation of herbicides. Operational variables and catalyst characterization assessment

Rafael R. Solís[a,b,*], F. Javier Rivas[a,b], Olga Gimeno[a,b] and Jose-Luis Pérez-Bote[c]

[a]Department of Chemical Engineering and Physical Chemistry, University of Extremadura, Av. Elvas s/n, 06006 Badajoz, Spain

[b]University Institute of Water Research, Climate Change and Sustainability, University of Extremadura, Av. Elvas s/n, 06006 Badajoz, Spain

[c]Department of Anatomy, Cellular Biology and Zoology, University of Extremadura, Av. Elvas s/n, 06006 Badajoz, Spain

*Department of Chemical Engineering and Physical Chemistry, University of Extremadura, Av. Elvas s/n, 06006 Badajoz, Spain. Email: rrodrig@unex.es

Abstract

BACKGROUND. This paper reports the use of novel coupled $LaCoO_3$-TiO_2 as photocatalyst with double route of peroxymonosulfate (PMS) activation. Firstly, as a photocatalyst due to titania; and secondly, through PMS heterogeneous decomposition onto $LaCoO_3$ particles. Thus, photocatalytical activity was tested for removing a mixture of four herbicides of different recalcitrance (metazachlor, tembotrione, tritosulfuron and ethofumesate).

RESULTS. The presence of light and PMS highly enhances herbicides rate removal. 3.5-5 times of increase were appreciated because of UVA light. Oxidant concentration, catalyst load, pH and temperature were assessed. Herbicides were completely oxidized depending on the operational variables and their recalcitrant nature. 55% of TOC conversion was reached using Oxone® 5 10^{-4} M. Phytotoxicity assays denoted no

inhibition after 180 min of photocatalytic treatment (~80% of initial inhibition). Solid properties of Co/Ti=0.1:1 ratio were studied by means of SEM ($LaCoO_3$ aggregates linked to a variety of shapes and sizes of TiO_2), XRF (6.1% of $LaCoO_3$), XPS (superficial Co^{3+}, La^{3+} and Ti^{4+}), XRD (anatase, rutile and rhombohedral $LaCoO_3$) and UV-vis reflectance (visible range absorption and bandgap of 2.88 eV for TiO_2).

CONCLUSION. Catalysts based on $LaCoO_3$-TiO_2 combined to peroxymonosulfate seem to be suitable for removing organic pollutants, with a moderate conversion of TOC and elimination of toxicity.

Keywords: photocatalysis, advanced oxidation, environmental remediation, heterogeneous catalysis, oxidation, decontamination

INTRODUCTION

Aqueous contaminants represent an environmental hazard since most of them are persistent and not easily removed by themselves in natural ecosystems. Pesticides are frequently detected in watercourses at low levels that risk non-compliance with European water framework Directive 2000/60/EC[1] drawn up to protect surface and ground waters.[2-3] Metazachlor (METAZ, $C_{14}H_{16}ClN_3O$, CAS 67129-08-2), tembotrione (TEMB, $C_{17}H_{16}ClF_3O_6S$, CAS 335104-84-2), tritosulfuron (TRITO, $C_{13}H_9F_6N_5O_4S$, CAS 142469-14-5) and ethofumesate (ETHO, $C_{13}H_{18}O_5S$, CAS 26225-79-6) are three different pesticides, with a relatively new presence in herbicide's market, which are used as pre and post-emergence herbicide to control a broad spectrum of broad-leaved and grassy weeds in crops, ornamental trees and shrubs. All of them, except tembotrione, are labelled as carcinogens. Moreover, tritosufuron and ethofumesate seem to have mutagenic action, and tritosulfuron is also an endocrine disrupter.[4] Some of

them, like ethofumesate, have been recently detected in surface and ground water[5] or soil.[6]

Management of organic aqueous pollutants is a matter of concern to water companies that need to develop new and specific technologies for that purpose. Conventional biological treatment seems to be inefficient due to the organic recalcitrant nature of these substances.[7-8] That is why alternative technologies such as chemical oxidation through Advanced Oxidation Processes are required. Peroxymonosulfate (PMS) is an oxidant which is attracting attention. This substance can be used as a promoter of sulfate radicals which present diverse advantages upon hydroxyl radical generation. Sulfate radical has a higher oxidation potential, more selectivity through electron transfer to chemicals that contains unsaturated bonds or aromatic rings, wider range of pH work in contrast to Fenton's chemistry, and higher half-life period which improves contact with the target compound. Furthermore, PMS decomposition provide both, sulfate and hydroxyl radicals.[9]

PMS by itself is poorly capable of attacking organic compounds at some points such as double bonds or aromatic rings;[10] however, its decomposition promoted by homogeneous or heterogeneous metallic catalysts, temperature, UV radiation, or ultrasound, considerably improve the elimination rate of organic pollutants. Homogeneous catalysis has the disadvantage of catalyst elimination and recycling after reaction, especially in those cases where its presence is undesirable, e.g. toxicological concerns. Some alternatives have been recently suggested. Heterogeneous catalysis combined with or without radiation,[11-12] has raised attention of diverse researching groups, mainly focusing on cobalt oxides.[13] Among them, heterogeneous combination with photocatalysts, such as titanium dioxide,[14-15] is drawing attention due to

enhancement in PMS decomposition. Cobalt joint to the titania acts as active center in PMS decomposition:[11]

$$Co^{2+} + HSO_5^- \rightarrow Co^{3+} + SO_4^{\bullet -} + HO^- \quad (1)$$

$$Co^{3+} + HSO_5^- \rightarrow Co^{2+} + SO_5^{\bullet -} + HO^- \quad (2)$$

Photocatalytic decomposition of PMS can also be launched under the presence of radiation and a photocatalyst:[15]

$$TiO_2 + h\nu \rightarrow e_{CB}^- + h_{VB}^+ \quad (3)$$

$$HSO_5^- + e_{CB}^- \rightarrow SO_4^{\bullet -} + HO^- \quad (4)$$

$$HSO_5^- + e_{CB}^- \rightarrow SO_4^{2-} + HO^{\bullet} \quad (5)$$

$$H_2O + h_{VB}^+ \rightarrow HO^{\bullet} + H^+ \quad (6)$$

Moreover electrons generated in photocatalytic processes contribute to regenerate the original oxidation state of cobalt, minimizing electron-hole recombination:[15]

$$Co^{3+} + e_{CB}^- \rightarrow Co^{2+} \quad (7)$$

$$Co^{2+} + h_{VB}^+ \rightarrow Co^{3+} \quad (8)$$

Thus, a powerful reaction-chained mechanism is triggered, generating sulfate and hydroxyl radicals from photocatalytic reaction and Fenton-like heterogeneous reactions. It should be highlighted that few new catalysts different from cobalt oxide have been coupled to TiO_2.[16-17]

This study reports the performance of lanthanum cobalt perovskite coupled to titania ($LaCoO_3$-TiO_2) as a new catalyst which combines heterogeneous and photocatalytic decomposition of PMS. The PMS catalytic decomposition through catalytic reactions

(1) and (2) using $LaCoO_3$ has been studied in a previous work, proving its high effectiveness, stability and low cobalt leaching under circumneutral pH range.[18] The purpose of the current work is to combine heterogeneous cobalt activity of $LaCoO_3$ and photocatalytic activity of TiO_2 in order to enhance the oxidation of organics pollutants, in this case a mixture of four new herbicides with high environmental concern. $LaCoO_3$:TiO_2 proportion influence on catalytic activity has been studied, being Co/Ti=0.1:1 chosen for the rest of the study. Main operational parameters such as PMS concentration, catalyst load, pH and temperature affecting herbicides' removal rate were considered. Catalyst stability was evaluated in consecutive runs of reusing. Phytotoxicity assays were carried out in order to assess the toxicological aspects of remaining TOC. Finally, main superficial properties of ratio Co/Ti=0.1:1 were analyzed through diverse techniques: SEM, XRF, XPS and UV-vis diffuse reflectance.

EXPERIMENTAL

Chemicals

All chemicals used were analytical grade and were used as received. Herbicides standards (purity >99%) were purchased from Sigma-Aldrich®. Oxone®, peroxymonosulfate compound ($2KHSO_5 \cdot KHSO_4 \cdot K_2SO_4$, CAS 37222-66-5), was obtained from Sigma-Aldrich®. The rest of chemicals used in catalyst synthesis were pure grade. Acetonitrile from VWR Chemicals was used in HPLC determination of herbicides in water. All solutions were prepared with ultrapure water from a Mili-Q® academic (Millipore) system (resistivity 18.2 MΩ cm).

Catalyst synthesis and characterization

$LaCoO_3$-TiO_2 was prepared in two different steps. Firstly, $LaCoO_3$ perovskite was synthetized in the presence of citric acid as complexing organic agent.[19] In a typical

synthesis run, $La(NO_3)_3 \cdot 6H_2O$ and $Co(CH_3COO)_2 \cdot 4H_2O$ with a molar ratio La:Co=1:1 were dissolved in 400 mL of ultrapure water. After 1 hour of mixing under magnetic agitation, 100 mL of citric acid in excess, twice the stoichiometrically needed for each metal, was slowly added. The resultant solution was heated at 100°C to remove water excess, drying thereafter the obtained pinkish gel. The solid was grinded and calcined at 700°C for 5 hours.

$LaCoO_3$-TiO_2 heterojunction was prepared by hydrothermal precipitation of a titanium organic precursor in the presence of the previous synthetized perovskite. Titanium isopropoxide was dissolved in 2-propanol and a fixed amount of $LaCoO_3$ was added under stirring to meet a specific $LaCoO_3$:TiO_2 molar ratio. Afterwards, ultrapure water was gradually dropped into the above suspension. The precipitation of titanium dioxide was completed by autoclaving the mixture at 80°C for 12 h. The resultant suspension was centrifuged at 3500 rpm and the solid washed with water and 2-propanol. Finally, the solid dried overnight at 100°C, was calcined at 500°C for 4 hours under air atmosphere (initial ramp, 10°C min^{-1}).

Mass titration method was considered to estimate pH of point of zero charge (pH_{pzc}).[20] A solution of pH=3 was prepared by adding NaOH 0.1 M to a HNO_3 0.1 M solution. Different glass bottles of 30 mL of capacity were filled in with 15 mL of the above solution, and different amounts of catalyst were added to meet a certain solid mass percentage (0.05, 0.10, 0.50, 1.00, 2.50, 5.00 and 10.00%). After 48 hours of equilibrium in a shaking water bath (25°), pH was measured. A plot of pH versus solid percentage gives a curve whose asymptote tends to be pH_{pzc} value.

Scanning electron microscopy (SEM) was conducted in a QUANTA 3D FEG (FEI) coupled to secondary and backscattered electrons detectors (acceleration voltage 20 kV).

XPS K-alpha-Thermo Scientific device was used for obtaining X-ray photoelectron spectroscopy (XPS) spectra, working with a Kα monochromatic source of Al (1486.68 eV). 284.8 eV for C 1s peak was taken to calibrate the signals of the rest peaks. High resolution of XPS spectra for La3d, Co2p, Ti2p and O1s were recorded.

Atomic concentration of La, Co and Ti were quantified by X-ray fluorescence (XRF) in a sequential Wavelength Dispersive X-ray Fluorescence (WDXRF) spectrometer (S8 Tigger, Brucker) equipped with an X-ray tube of rhodium (60 kV, 170 mA).

Crystalline phase composition was analyzed by X-ray diffraction (XRD), in a Bruker D8 Advance diffract meter equipped with a monochromator of Ge 111 Kα of Cu (wavelength, 1.5456 Å).

Diffuse reflectance UV-Vis spectra was performed by using a Varian-Agilent UV-Vis-NIR Caty 5000 spectrophotometer, equipped with an integrating sphere device.

Photoreactor and procedure

Experimental photoreactor setup consisted of a cylindrical glass vase (10 cm of diameter and 22 of height) in which 1.0 L of herbicides mixture (1 mg L^{-1} of each) was loaded. The reactor was magnetically stirred and thermally controlled by using an IKA® RCT basic stirrer. The installation was completed with a 31 cm external diameter pipe of 54 cm of height, being the reactor located in the center. Four tubular black light lamps (41 cm of height, LAMP15TBL HQPOWERTM manufactured by Velleman®, 15 W of nominal power) were equidistantly distributed and attached to the internal wall of the pipe, which was foiled by aluminum foil. Every lamp mainly emits radiation within the range 350-400 nm, with a maximum placed at 365 nm. Figure S1, available in supplementary information, provides a scheme of the photoreaction system and Figure S2 the emission spectrum of UVA lamp.

Previous to the experiment, pH (measured by a Crison GLP 21+) was adjusted to the specific value and 30 min of stirring without PMS was carried out in order to achieve the adsorption equilibrium of organic compounds onto catalyst surface (if any). A small volume (less than 10 mL) of a concentrated PMS solution was added in order to meet the PMS initial concentration and to start the reaction. Then pH was quickly readjusted. Samples were extracted at different times and filtered with Millex-HA filters (Millipore, 0.45 μm). HPLC and TOC samples were quenched with $Na_2S_2O_3$ 0.5 M (10μL per 1 mL of sample).

Analytical methods

PMS concentration was spectrophotometrically quantified by means of a method based on *N,N*-diethyl-p-phenylenediamine (DPD) oxidation.[21]

Herbicides aqueous concentration were analyzed by liquid chromatography in a HPLC Agilent 1100 equipped with UV detection. A Kromasil 100 5C18 column (5μm, 2.1x150 mm) was used, and a mobile phase composed by 0.1% H_3PO_4 acidified water (A) and acetonitrile (B) was pumped at a flow rate of 1 mL min^{-1}, with an isocratic percentage composition of 55:45 A:B. UV detection was conducted at 220 nm.

Total Organic Carbon (TOC) content was determined by means of a Shimazdu TOC-V_{CSH} 5000A analyzer which directly injects the aqueous sample.

The Ionic Chromatographic system was a Methrom® 881 Compact IC pro equipped with 800 Dosino, chemical suppression, autosampler (863 Compact autosampler) and conductivity detector. The stationary phase was an anionic-exchange column (MetroSep A Supp 5).

Cobalt in solution was measured through atomic absorption in a Varian SpectrAA Series 140 device.

Phytotoxicity assays were carried out with seeds of *Lactuca Sativa* as test plant (*Romana Bionda Degli Ortolani*, Vilmorin®). Fifteen seeds were equally distributed into Petri dishes equipped with paper discs moistened with 4 mL of sample. Paraffin was used to cover the dishes in order to avoid liquid evaporation, and the seeds were incubated in a germination chamber, isolated from light at 22°C during 120 hours. After that, the root length of each germinated root was measured (L), expressed as the sum of hypocotyl and radicle. The percentage root growth was calculated by comparing the radicle lengths for each sample with those observed in the control (L_0), done with ultrapure water.

RESULTS & DISCUSSION

Effect of the ratio $LaCoO_3$:TiO_2

Different catalysts were tested varying the ratio of the perovskite to titanium dioxide. Also, pure TiO_2 and $LaCoO_3$ were also used as control runs to have a reference in activity. The first case represents the conventional photocatalytic process in the presence of a promoter. The second case reveals the capacity of the perovskite to decompose peroxymonosulfate. Fig. 1 shows the results obtained.

At the sight of Fig. 1, depending on the herbicide the optimum catalyst is different. As a rule of thumb, catalysts with Co:Ti ratios in the range 0.1:1 to 0.5:1 show a higher activity than the rest of solids tested. Titanium dioxide displays moderate activity with the exception of ethofumesate. In the latter case, TiO_2 leads to the highest herbicide conversion after 60 minutes (around 70% conversion of the initial ethofumesate concentration). Tembotrione is one of the most reactive herbicides tested, in this case, even peroxymonosulfate in the absence of radiation and catalyst is capable of oxidize the herbicide.

Additionally, no matter the ratio Co:Ti used, a fast initial period in herbicide elimination was experienced followed by a second slower stage. An analysis of Oxone® evolution (results not shown) reveals that the slow stage does not coincide with peroxymonosulfate total depletion. A potential explanation could be a shortage in dissolved oxygen that would prevent the propagation of the free radical mechanism through organoperoxides radical formation/decomposition.[22] Also, electron-hole recombination is favored in the absence of oxygen. As a consequence, a new experimental series was conducted by injecting an oxygen stream to the reaction media.

Fig. 2 illustrates that oxygen has no influence in the process with the exception of tembotrione. In this latter case the concentration of O_2 exerts a positive influence; however, given the high reactivity of tembotrione and the residual improvement obtained in terms of total conversion of herbicides, it was decided to continue this study in the absence of oxygen, avoiding, therefore, additional costs associated to the process.

Peroxymonosulfate concentration effect

Given the results obtained in the previous section, the catalyst with a ratio Co:Ti of 0.1 was thereafter used in the rest of experiments. This catalyst represents a compromise between conversion achieved and low cobalt content to avoid leaching of this transition metal.

The next experimental series was conducted at different initial Oxone® concentrations and keeping constant the rest of operating variables. Additionally, some control runs have also been conducted.

Fig. 3 illustrates the results obtained. For comparison purposes, from the same figure, the role played by Oxone® alone is shown. At this point it should be highlighted that in a previous work,[23] only tembotrione presented some reactivity towards Oxone® in

experiments carried out individually. However, when treating the four herbicides simultaneously, conversions of 78, 53, 3 and 21% in metazachlor, tembotrione, tritosulfuron and ethofumesate were experienced after 180 min. It seems that either species formed in the oxidation of tembotrione by Oxone® have the capacity to co-oxidize the rest of herbicides or/and at pH=7, herbicides are more reactive towards peroxymonosulfate than at pH=3 used in the reference. A first approximation to peroxymonosulfate oxidation kinetics can be accomplished by considering a second order reaction:

$$-\frac{dC_{Herbicide}}{dt} = k_{PMS} C_{Herbicide} C_{PMS} \quad (9)$$

where $C_{Herbicide}$ and C_{PMS} mean the concentration of herbicide and PMS, respectively; and k_{PMS} the second order pseudo rate constant. Applying equation 9 to experiments displayed in Fig. 3 led to k_{PMS} values of 75.1 ± 7.3, 50.2 ± 5.2, 2.0 ± 0.6, and 15.1 ± 1.8 M^{-1} min^{-1} (corresponding to metazachlor, tembotrione, tritosulfuron, and ethofumesate removal, respectively), where herbicides concentration was monitored in mg L^{-1} and PMS concentration in mol L^{-1}. Given the values of k_{PMS}, the most recalcitrant compound is tritosulfuron while the most reactive is metazachlor. Notice that in individual experiments metazachlor did not react with peroxymonosulfate at pH=3.

The presence of light and PMS involves a considerable enhancement of the process. This improvement is not the consequence of the direct activation of peroxymonosulfate by UVA radiation. At 365 nm nor PMS nor the herbicides absorb radiation (see supplementary information, Fig. S2). Likely, herbicides act as sensitizers of the photoreaction initiating the mechanism of photodecomposition of peroxymonosulfate. Again, for comparison purposes the global process was modeled by a second order expression, similar to Eq. 9 leading to values of the rate constant of $k_{PMS, UVA}$ = 0.350 ±

1 0.04 10^3, 0.175 ± 0.028 10^3, 8.5 ± 1.1, and 75 ± 5.3 M^{-1} min^{-1} (metazachlor,
2 tembotrione, tritosulfuron, and ethofumesate). As inferred from these values, the
3 presence of light increased the reactivity in the range of 3.5-5 times if compared to
4 experiments in the absence of radiation. $LaCoO_3$ does not have photocatalytic activity
5 by itself, fact that was proved by carrying out an experiment in absence of PMS (results
6 not shown). In a similar way, TiO_2 shows is capable of oxidizing herbicides at similar
7 rate constant to direct oxidation with Oxone®, as it can be appreciated in Fig. 3.

8 When the $LaCoO_3$-TiO_2 catalyst was added to the reaction media, PMS concentration
9 exerted a positive influence in herbicides removal rate. An initial concentration of the
10 promoter of 5 10^{-4} M led to the instantaneous removal of three of the four compounds,
11 tritosulfuron was eliminated after roughly 2 hours. Maximum TOC conversion after 180
12 min was 55%. At the sight of the profiles obtained and the low TOC reduction,
13 accumulation of intermediates is likely to occur impeding the adsorption of reactants
14 onto the catalyst surface and competing for oxidizing species. Moreover, curve shapes
15 rule out the development of simple second order kinetics. Accordingly, a rough
16 empirical approximation to the kinetics of the process would consider that the rate of
17 any herbicide removal would be proportional to the amount of the parent compound,
18 catalyst load and the concentration of reactive species, and inversely proportional to the
19 amount of intermediates generated. Some of the previous parameters have not been
20 monitored in this study, however, for comparison purposes a pseudoempirical model
21 can be proposed by considering that oxidizing species are proportional to PMS
22 concentration and intermediates accumulation is proportional to reaction time:

23
$$-\frac{dC_{Herbicide}}{dt} = k(T,Cat,UVA,pH)\frac{C_{Herbicide}\left(\sum C_{Oxidants}\right)}{\sum C_{Intermediates}} \approx \approx k(T,Cat,UVA,pH)\frac{C_{Herbicide}C_{PMS}}{t^n} \quad (10)$$

In equation 10, herbicides concentration has been measured in mg L^{-1} and PMS in mol L^{-1}. Time in minutes is powered to "n". The rate constant is a function of temperature, catalyst load, UVA radiation and geometry of the reactor, and likely, of pH. Applying the Euler approximation to the derivative term:

$$C_{i+1,\,Herbicide} = C_{i,\,Herbicide} - \left(k(T,Cat,UVA,\,pH)\frac{C_{i,\,Herbicide}\left(\sum C_{i,\,oxidants}\right)}{\sum C_{i,\,Intermediates}} \right)\Delta t \approx$$
$$\approx C_{i,\,Herbicide} - \left(k(T,Cat,UVA,\,pH)\frac{C_{i,\,Herbicide}C_{i,\,PMS}}{t_i^n} \right)\Delta t \qquad (11)$$

Where C_i is the concentration at time i, and C_{i+1} refers to the concentration at time $i+\Delta t$. The optimization process that minimized the squared difference between calculated and experimental concentrations led to values of n in the range 0.5-0.8, however, for comparison purposes in terms of reactivity of herbicides, in this first series, this parameter was fixed to 0.8 in all experiments. The rate constants k were $4.8 \pm 0.1\ 10^3$, $3.9 \pm 0.2\ 10^3$, $5.9 \pm 1.1\ 10^2$, and $2.6 \pm 0.3\ 10^3\ M^{-1}\ min^{-0.2}$, corresponding to metazachlor, tembotrione, tritosulfuron, and ethofumesate removal, respectively. As seen in Fig. 3, equation 10 is a suitable tool to compare the reactivity of the different herbicides under a variety of experimental conditions. In this case, the most reactive substance is metazachlor while tritosulfuron is almost 10 times more recalcitrant than the former.

The presence of cobalt in the catalyst is of paramount importance. Hence, Fig. 3 displays how, under similar experimental conditions, the removal rate of herbicides diminishes when only TiO_2 was present if compared to the similar experiment completed with the $LaCoO_3$-TiO_2 catalyst. Also, the accumulation of intermediates affects to a lower extent the conversion of the herbicides at higher reaction times. As a consequence, when TiO_2 was used, the curve profiles were different to those experienced when the $LaCoO_3$-TiO_2 catalyst was employed. Hence, the initial oxidation

rate was slower in TiO_2 based experiments, however, this reaction rate did not suffer a sharp decrease at higher reaction times as in the case of the perovskite based solid. An expression similar to equation 11 was adopted to model the process. With the exception of tritosulfuron, the model led to acceptable results. As deduced from the curve shapes the value of "n" decreased from 0.8 to 0.4 indicating the lower effect of intermediates on catalyst activity. Simultaneously, the values of the rate constants also diminished to values of $2.2 \pm 0.6\ 10^3$, $1.0 \pm 0.08\ 10^3$, and $0.95 \pm 0.04\ 10^3$ M^{-1} $min^{-0.6}$ for metazachlor, tembotrione, and ethofumesate, respectively.

Influence of catalyst concentration

The influence of catalyst concentration was investigated in the range 0.05 to 0.5 g L^{-1}. Fig. 4 depicts the results obtained. As inferred from the figure, no significant influence was observed and herbicide conversion was almost similar regardless of the amount of catalyst used in the interval studied. Catalyst dosage did affect the PMS decomposition rate. Hence, the higher amount of catalyst, the faster decomposition of peroxymonosulfate. However, as stated previously, this decomposition does not lead to a better performance in terms of herbicides or TOC removal.

pH influence

pH influence was assessed from slightly acidic conditions (pH=5) to slightly basic conditions (pH=8). pH plays a notorious role in the chemistry of peroxymonosulfate decomposition. Fig. 5 shows the results obtained. As observed, pH exerts a notorious influence in the herbicides removal rate. Total organic carbon elimination, however, was similar regardless of the pH (roughly 30% conversion after 180 min).

As inferred from Fig. 5, the best conditions were obtained at the lowest pH used. One of the reasons to explain the results could be the influence of leached cobalt into solution.

Cobalt above the detection limit of the analytical procedure used was only detected at pH=5. Under these conditions the maximum amount of Co was 0.8 mg L^{-1} (1.4 10^{-5} M) at 180 min. Some experiments carried out in homogenous mode revealed that this small amount was insufficient to explain the effect of pH and/or the activity of the tested catalyst. In most cases, equation 10 could acceptably simulate the curve profiles obtained. The optimum value of n was 0.8 for metazachlor and 0.5 for the rest of herbicides. pH negatively affected the values of k. Table 1 shows the values obtained as a function of pH.

The tendency here obtained coincides with those reported when the perovskite $LaCoO_3$ was used in the presence of Oxone® to treat these herbicides.[18] Apparently, the dissociation degree of peroxymonosulfate (pKa = 9.4) highly influences its decomposition onto the catalyst surface. The catalyst has a point of zero charge around 6.22, suggesting that the solid presents low affinity towards negative ionic species.

Temperature influence

The effect of temperature was investigated by using two different initial PMS concentrations, 2.0 and 3.0 10^{-4} M. Fig. 6 illustrates the results obtained in experiments completed with the lowest PMS concentration in the range 30-50°C. Insets contain the Arrhenius plot derived from calculated rate constants.

As expected, temperature exerts a positive influence in the process; however, the values of the activation energy obtained are not excessively high, indicating that this parameter does not produce notable modifications in the efficacy of the process, at least in the range of temperatures investigated. Calculated activation energies were 14.7 (R^2 = 0.96), 20.5 (R^2 = 0.96), 20.5 (R^2 = 0.98) and, 28.7 (R^2 = 0.99) kJ mol^{-1} corresponding to metazachlor, tembotrione, tritosulfuron, and ethofumesate, respectively. Higher

temperatures (above 80°C) might lead to the thermal decomposition of PMS into radicals. In this case, temperature influence could be different.[24]

Catalyst stability

Catalyst stability was assessed by conducting several consecutive experiments using the same recycled catalyst after filtration and drying. Fig. 7 shows the evolution of Oxone® decomposition with time in the aforementioned experiments. The calculated reaction rate constant according to equation 10 is also depicted for each cycle. At the sight of Fig. 7, a slight decrease in peroxymonosulfate decomposition rate can be envisaged as the number of reuses is augmented; however, this reduction is not translated to a deterioration of the process efficiency. Actually, with the exception of tritosulfuron, calculated rate constants maintain, or even increase, the values obtained when fresh catalyst was used. In the case of tritosulfuron, the rate constant is reduced from the control run (fresh catalyst) to the first cycle; thereafter, this constant does not suffer any appreciable change. The reason is unclear and needs further work; in all cases leached cobalt was negligible.

Phytotoxicity evolution

Previous experiments have revealed that herbicides can be easily removed from water if adequate conditions are applied. However, no total mineralization of the samples could be achieved. Accordingly, this section was devoted to assess the potential phytotoxicity of the accumulated intermediates during the photocatalytic oxidation in presence of Oxone®.

Hence, a series of experiments were conducted in the presence of radiation and different amounts of Oxone®. Thereafter, seeds of *Lactuca Sativa* were germinated as described in the experimental section. Fig. 8 illustrates the results of root length obtained when

germinating the seeds in water samples extracted at different reaction times. As observed, when no treatment is applied (time zero), root growth only achieves ~20% (~80% of inhibition) of the root length obtained with pure water. As the reaction exposure increases, phytotoxicity almost disappears. Hence, the higher the initial PMS amount used, the faster the phytotoxiciy decreases. With the exception of the run conducted with the lowest PMS concentration, all samples did show no phytotoxicity after 180 min of treatment.

Although organic intermediates have not been measured in this work, some ionic species were detected and monitored throughout the reaction by ionic chromatography. In this sense, several aspects can be highlighted. Hence, the F-C bond is hardly broken in $-CF_3$ substituents; the amount of free fluoride found in most cases was below the 10% of the maximum concentration that could be released. Nitrates were found at maximum concentrations around 18% of the highest concentration that could be found. This quantity coincides with the amount of nitrates that would be generated from the two amine groups in tritosulfuron, i.e. nitrogen in the heterocycle seems to be difficult to be converted to inorganic nitrate. Amongst small organic acids, acetic, formic, succinic and muconic acids were tentatively detected. Fig. 9 shows the evolution of acetic and formic acids.

Catalyst characterization

Once the performance of the catalyst was assessed, the catalyst with the ratio Co/Ti= 0.1:1 used in most of experiments was characterized by means of several techniques.

Fig. 10 summarizes some of the SEM images obtained. A, B and C pictures were obtained with secondary electron detection, while A', B' and C' are their corresponding images acquired with BackScattered Electron (BSE). More detailed pictures can be

observed in supplementary information, Fig. S3. From Fig. 10 can be appreciated a variety of sizes (from 20 to less than 5 μm) and shapes likely due to irregularity of titania particles. From BSE images brighter particles outstand from the rest. These highlighted regions, which usually correspond to heavy elements, represent aggregates of smaller spherical $LaCoO_3$ particles. Energy Dispersive X-ray (EDX) analysis led to the confirmation of composition (Table S1), enabling the corroboration that the darkest particles of BSE images belong to titania while the brightest correspond to perovskite.

X-ray Fluorescence (XRF) technique made possible to obtain global percentages of each element, and not only superficial. In this way, mass percentage of each element, without considering oxygen, were 80.41, 12.63 and 5.72 for Ti, La and Co, respectively. In a $LaCoO_3$ structure atomic mass relation between composition percentages of La and Co is La/Co=2.36, while in the synthesized $LaCoO_3$-TiO_2 this relation is 2.20. This near proportion might be considered as a proof of perovskite presence. Moreover, if it is considered that for a 10% of $LaCoO_3$ in the structure of the catalyst, mass percentage of La must be 20.55; a 6.1% of molar perovskite is found in the synthesized solid.

Surface composition and oxidation state of each element were analyzed by means of XPS. Figure 11 summarizes the results of general spectrum and high resolution spectra for La3d, Co2p, Ti2p and O1s. On one hand, Co and La present trivalent oxidation states. Co2p image depicts two peaks at 794.1 and 779.4 eV, corresponding to $Co2p_{1/2}$ and $Co2p_{3/2}$ respectively. The value observed for $Co2p_{3/2}$ matches with that observed in cobalt oxides such as Co_2O_3[25] and $LaCoO_3$,[26] where Co(III) is the main oxidation state. La3d presents two regions ($La3d_{5/2}$ and $La3d_{3/2}$), containing two peaks each one whose values are 834.7 and 839.0 eV for $La3d_{5/2}$ region; and, 851.4 and 856.0 eV for $La3d_{3/2}$. These values are consistent with that expected for trivalent La in $LaCoO_3$ network.[27] On the other hand, Ti2p peak showed the typical value when XPS is carried out in TiO_2.

Thus, Fig. 11 illustrates a symmetrical $Ti2p_{3/2}$ peak whose maximum is located at 458.8 eV. Finally, O1s presents a completely symmetrical peak at 529.9 eV, associated to O^{2-} state, which outlines the absence of hydroxylated groups onto the surface. A quantitative surface analysis, after Shirley's background subtraction, led to the following composition expressed as atomic percentages: 59.3 of O, 21.5 of Ti, 3.1 of La, and 4.36 of Co.

XRD technique was applied in order to study the nature of crystalline phases present in the catalyst. XRD patterns are presented in Fig. 12. Anatase and rutile were identified as the main TiO_2 oxides, being anatase 73.1% of all TiO_2. $LaCoO_3$ presence was confirmed as rhombohedral crystalline structure, as well as small amounts of cubic Co_3O_4.

Finally, optical absorbance was applied by means of diffuse reflectance UV-vis technique. Fig. 13 illustrates the spectra obtained and the corresponding Tauc's plot for bandgap determination. At first sight, absorption efficiency considerably increases in the visible range due to perovskite presence. Moreover, the $LaCoO_3$-TiO_2 presents two different absorption regions, whose bandgaps are 2.88 and 1.81 eV, being attributed to TiO_2 and $LaCoO_3$ respectively. Cobalt oxides combined with TiO_2 frequently has two bandgaps.[16] Titania synthesized by hydrothermal method usually presents value around 3.2 eV, not showing visible light absorption. Although a slight decrease of bandgap might be consequence of cobalt[15, 28] or lanthanum doping,[29] in this case this value drops to 2.88 eV, far from being explained by this effect. Presence of transition metal oxides coating TiO_2 has been reported to shift bandgap value of TiO_2.[30] Therefore, $LaCoO_3$-TiO_2 composite may be the origin of the bandgap decrease for TiO_2 reported in this study.

CONCLUSIONS

Catalysts based on $LaCoO_3$-TiO_2 seem to be suitable for removing organic pollutants through combination of photocatalytic and heterogeneous decomposition of peroxymonosulfate. Co/Ti ratio of 0.1:1 is enough to reach enhanced degradation rates if compared to bare titania or pure perovskite. From all variables assessed, oxone® concentration is the most influential, making possible to remove almost instantaneously herbicides at concentration up to 5 10^{-4} M of oxone®. Tritosulfuron was 10 times more recalcitrant than the rest. Maximum mineralization extent was found to be 55% (5 10^{-4} M oxone®, 3 hours of treatment), with low release of fluorine (~10%) and nitrate (~18%). Nevertheless, phytotoxicity assays of *Lactuca Sativa* germination pointed out almost complete disappearance in growth inhibition. Thus, the higher PMS amount used in the photocatalytic process, the faster phytotoxicity decreases during treatment.

$LaCoO_3$-TiO_2 (ratio Co/Ti=0.1:1) characterization by SEM indicated a heterogeneous variety of TiO_2 size and $LaCoO_3$ aggregates which seem to be made of smaller spheres. XRF technique led to quantification of roughly 6% of $LaCoO_3$ in the solid. Superficial XPS highlighted the oxidation states of Co^{3+}, La^{3+}, Ti^{4+}, O^{2-} and absence of hydroxyl groups. A high increase in absorption in the visible range is appreciated in UV-vis spectra, with bandgaps of 2.88 and 1.81 eV due to TiO_2 and $LaCoO_3$ particles, respectively.

Acknowledgements

Authors thank economic support received from Junta de Extremadura, CICYT of Spain and FEDER founds through Projects GR15033 and CTQ2015/64944-R, respectively. Mr. Rafael Rodríguez Solís also acknowledges Gobierno de Extremadura, Consejería de Empleo Empresa e Innovación, and FSE Funds for his Ph.D. grant (PD12058). Catalyst characterization was provided by Facility of Analysis and Characterization of Solids

and Surfaces of SAIUEx (financed by University of Extremadura, Junta de Extremadura, MICINN, FEDER and FSE).

References

1. Directive of the European Parliament and of the council 2000/60/EC establishing a framework for community action in the field of water policy. Official Journal C513, 23/10/2000.

2. Loos R, Gawlik BM, Locoro G, Rimaviciute E, Contini S and Bidoglio G, EU-wide survey of polar organic persistent pollutants in European river waters. *Environ Pollut* **157**:561-568 (2009).

3. R. Loos R, Locoro G, Comero S, Contini S, Schwesig D, Werres F, Balsaa P, Gans O,Weiss S, Blaha L, Bolchi M and Gawlik BM, Pan-European survey on the occurrence of selected polar organic persistent pollutants in ground water. *Water Res* **44**:4115-4126 (2010).

4. Pesticide Properties DataBase (PPDB). University of Hertfordshire, UK. http://sitem.herts.ac.uk/aeru/ppdb/en/index.htm, 2016 (last accessed 15.07.16).

5. Herrero-Hernández E, Andrades MS, Álvarez-Martín A, Pose-Juan E, Rodríguez-Cruz MS and Sánchez-Martín MJ, Occurrence of pesticides and some of their degradation products in waters in a Spanish wine region. *J Hydrol* **486**:234-245 (2013).

6. Pose-Juan E, Sánchez-Martín MJ, Andrades MS, Rodríguez-Cruz MS and Herrero-Hernández E, Pesticide residu*es* in vineyard soils from Spain: Spatial and temporal distributions. *Sci Total Environ* **514**:351-358 (2015).

7. Loos R, Carvalho R, António DC, Comero S, Locoro G, Tavazzi S, Paracchini B, Ghiani M, Lettieri T, Blaha L, Jarosova B, Voorspoels S, Servaes K, Haglund P, Fick J, Lindberg RH, Schwesig D and Gawlik BM, EU-wide monitoring survey on emerging

polar organic contaminants in wastewater treatment plant effluents. *Water Res* **47**:6475-6487 (2013).

8. Martínez Bueno MJ, Gomez MJ, Herrera S, Hernando MD, Agüera A and Fernández-Alba AR, Occurrence and persistence of organic emerging contaminants and priority pollutants in five sewage treatment plants of Spain: Two years pilot survey monitoring. *Environ Pollut* **164**:267-273(2012).

9. Hu P and Long M, Cobalt-catalyzed sulfate radical-based advanced oxidation: A review on heterogeneous catalysts and applications. *Appl Catal B* **181**:103-117 (2016).

10. Renganathan R and Maruthamuthu PJ, Kinetics and mechanism of oxidation of aromatic aldehydes by peroxomonosulphate. *J Chem Soc, Perkin Trans 2* **11**:285-289 (1986).

11. Yang Q, Choi H and Dionysiou DD, Nanocrystalline cobalt oxide immobilized on titanium dioxide nanoparticles for the heterogeneous activation of peroxymonosulfate. *Appl Catal B* **74**:170-178 (2007).

12. Yang Q, Choi H, Chen Y and Dionysiou DD, Heterogeneous activation of peroxymonosulfate by supported cobalt catalysts for the degradation of 2,4-dichlorophenol in water: The effect of support, cobalt precursor, and UV radiation, *Appl Catal B* **77**:300-307 (2008).

13. Anipsitakis GP and Dionysiou DD, Radical Generation by the Interaction of Transition Metals with Common Oxidants, *Environ Sci Technol* **38**:3705-3712 (2004).

14. Chen Q, Ji F, Liu T, Yan P, Guan W and Xu X, Synergistic effect of bifunctional Co–TiO_2 catalyst on degradation of Rhodamine B: Fenton-photo hybrid process. *Chem Eng J* **229**:57-65(2013).

15. Chen Q, Ji F, Guo Q, Fan F and Xu X, Combination of heterogeneous Fenton-like reaction and photocatalysis using Co–TiO_2 nanocatalyst for activation of $KHSO_5$ with visible light irradiation at ambient conditions. *J Environ Sci* **26**:2440-2450 (2014).

16. Sathishkumar P, Mangalaraja RV, Anandana S and Ashokkumar M, $CoFe_2O_4/TiO_2$ nanocatalysts for the photocatalytic degradation of Reactive Red 120 in aqueous solutions in the presence and absence of electron acceptors. *Chem Eng J* **220**:302-310 (2013).

17. Chan KH and Chu W, Degradation of atrazine by cobalt-mediated activation of peroxymonosulfate: Different cobalt counteranions in homogenous process and cobalt oxide catalysts in photolytic heterogeneous process. *Water Res* **43**:2513-2521 (2009).

18. Solís RR, Rivas FJ and Gimeno O, Removal of aqueous metazachlor, tembotrione, tritosulfuron and ethofumesate by heterogeneous monopersulfate decomposition on lanthanum-cobalt perovskites, *Appl Catal B* **200**:83-92 (2017).

19. Sotelo JL, Ovejero G, Martínez F, Melero JA and Milieni A, Catalytic wet peroxide oxidation of phenolic solutions over a $LaTi_{1-x}Cu_xO_3$ perovskite catalyst. *Appl Catal B* **47**:281-294 (2004).

20. Noh JS and Schwarz JA, Effect of HNO_3 treatment on the surface acidity of activated carbons. *Carbon* **28**:675-682 (1990).

21. Fukushima M and Tatsumi K, Effect of Hydroxypropyl-β-cyclo-dextrin on the Degradation of Pentachlorophenol by Potassium Peroxymonosulfate Catalyzed with Iron(III)−Porphyrin Complex. *Environ Sci Technol* **39**:9337-9342 (2005).

22. Rivas FJ, Beltrán FJ, Carvalho F and Álvarez PM, Oxone-Promoted Wet Air Oxidation of Landfill Leachates. *Ind Eng Chem Res* **44**:749-758 (2005).

23. Solís RR, Rivas FJ and Tierno M, Monopersulfate photocatalysis under 365 nm radiation. Direct oxidation and monopersulfate promoted photocatalysis of the herbicide tembotrione. *J Environ Manage* **181**:385-394 (2016).

24. Yang S, Wang P, Yang X, Shan L, Zhang W, Shao X and Niu R, Degradation efficiencies of azo dye Acid Orange 7 by the interaction of heat, UV and anions with common oxidants: persulfate, peroxymonosulfate and hydrogen peroxide. *J Hazard Mater* **179**:552-558 (2010).

25. McIntyre NS and Cook MG, X-ray photoelectron studies on some oxides and hydroxides of cobalt, nickel, and copper. *Anal Chem* **47**:2208-2213 (1975).

26. Yang Z, Huang Y, Dong B, Li HL and Shi SQ, Sol–gel template synthesis and characterization of $LaCoO_3$ nanowires. *Appl Phys A Mater Sci Process* **84**:117-122 (2006).

27. Natile MM, Ugel E, Maccato C and Glisenti A, $LaCoO_3$: Effect of synthesis conditions on properties and reactivity. *Appl Catal B* **72**:351-362 (2007).

28. Jiang P, Xiang W, Kuang J, Liu W and Cao W, Effect of cobalt doping on the electronic, optical and photocatalytic properties of TiO_2. *Solid State Sci* **46**:27-32 (2015).

29. Liqiang J, Xiaojun S, Baifu X, Baiqi W, Weimin C and Honggang F, The preparation and characterization of La doped TiO_2 nanoparticles and their photocatalytic activity. *J Solid State Chem* **177**:3375-3382 (2004).

30. Pozan GS, Isleyen M and Gokcen S, Transition metal coated TiO_2 nanoparticles: Synthesis, characterization and their photocatalytic activity. *Appl Catal B* **140-141**:537-545 (2013).

Table 1. Rate constants (x 10^{-3}) calculated for herbicides elimination (M^{-1} min^{n-1}) as a function of pH (n = 0.8 for metazachlor and n= 0.5 for the rest of compounds).

	Metazachlor	**Tembotrione**	**Tritosulfuron**	**Ethofumesate**
pH=5	-	-	4.6 ± 0.1	-
pH=6	-	-	2.8 ± 0.1	9.0 ± 0.3
pH=7	6.0 ± 0.3	3.1 ± 0.4	0.55 ± 0.08	2.1 ± 0.2
pH=8	4.1 ± 0.4	1.2 ± 0.4	0.22 ± 0.02	0.95 ± 0.12

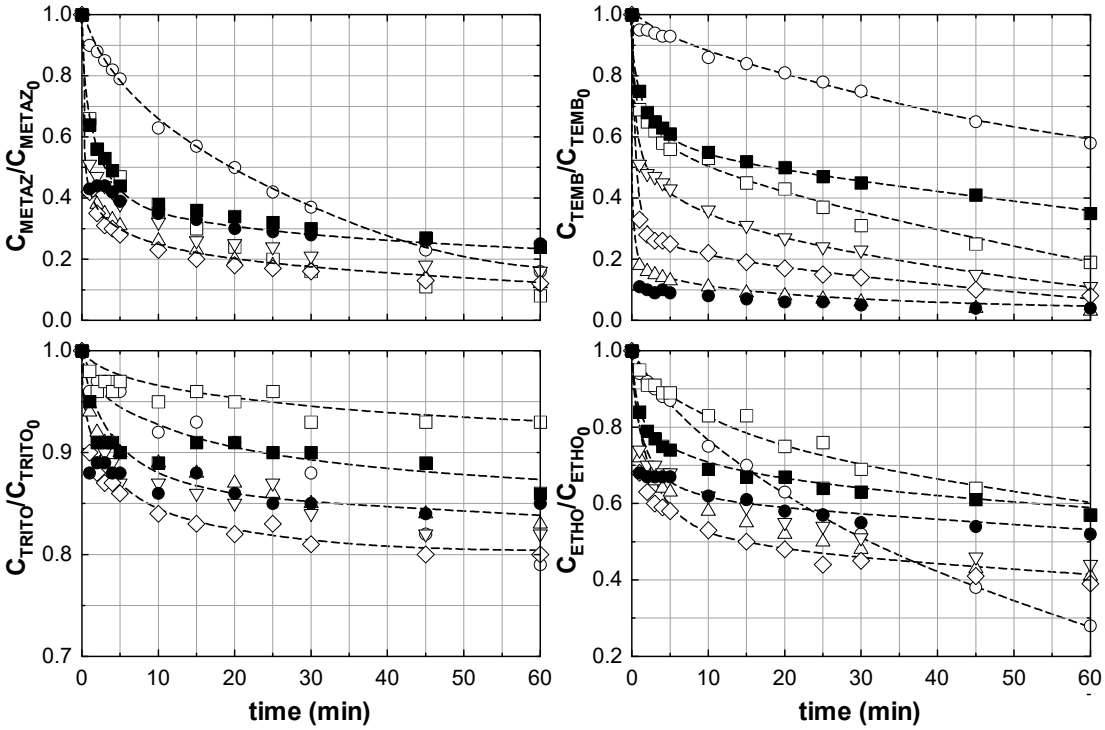

Fig. 1 Oxone® promoted photocatalytic elimination of herbicides. $LaCoO_3$-TiO_2 ratio influence. Experimental conditions: $C_{Herbicide}$ = 1.0 mg L^{-1} each, pH = 7.0, T = 15-20°C, C_{CAT}= 0.5 g L^{-1}, $C_{Oxone®}$ = 1.0 10^{-4} M. Ratio Co/Ti: ○, 0:1; □, 0.05:1; Δ, 0.1:1; ∇, 0.25:1; ◊, 0.5:1; ●, 0.75:1; ■, 1:0.

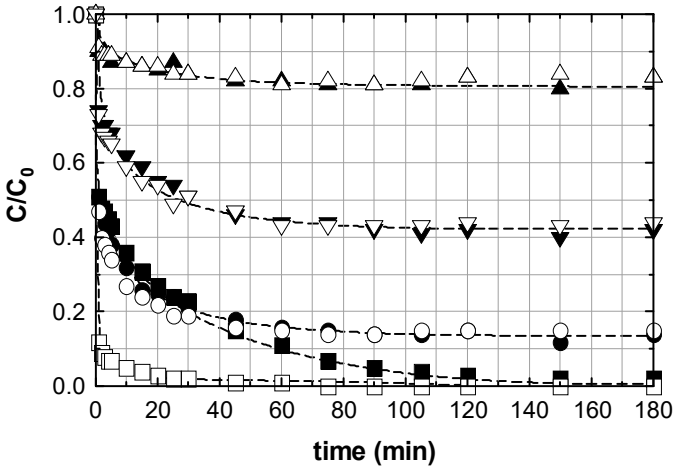

Fig. 2 Oxone® promoted photocatalytic elimination of herbicides. Oxygen bubbling effect. Experimental conditions: $C_{Herbicide}$ = 1.0 mg L^{-1} each, pH = 7.0, T = 15-20 °C, C_{CAT} = 0.5 g L^{-1}, $C_{Oxone®}$ = 1.0 10^{-4} M, Ratio Co/Ti= 0.25:1. ●○, Metazachlor; ■□, Tembotrione; ▲Δ, Tritosulfuron; ▼∇, Ethofumesate. (Open symbols: oxygen bubbling, Solid symbols: air bubbling).

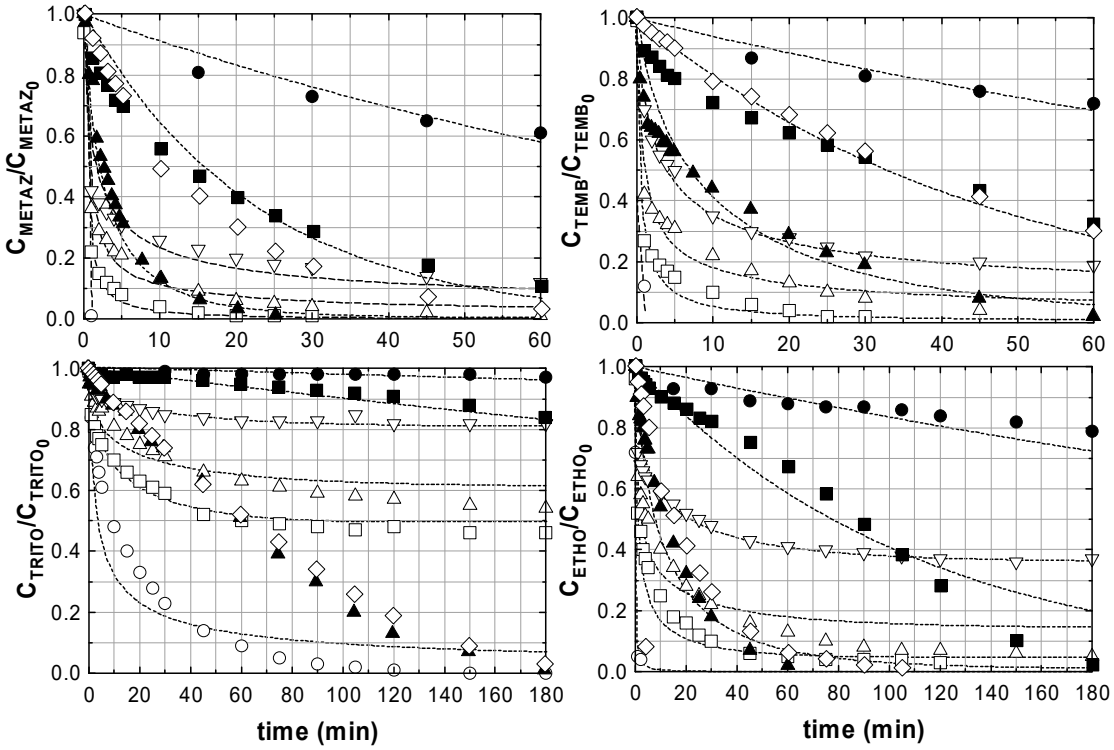

Fig. 3 Oxone® promoted photocatalytic elimination of herbicides. Oxone® concentration influence. Experimental conditions: $C_{Herbicide}$ = 1.0 mg L^{-1} each, pH = 7.0, T = 15-20 °C, C_{CAT}= 0.5 g L^{-1}, Ratio Co/Ti= 0.1:1, $C_{Oxone®} \cdot 10^4$ (M): ○, 5.0; □, 2.0; Δ, 1.5; ∇, 1.0; ●, 1.5 (no UVA, no catalyst); ■, 1.5 (no catalyst); ▲, 5.0 (Ratio Co/Ti= 0:1); ◊, 0 (Ratio Co:Ti=0:1). Dashed lines: theoretical calculations with n = 0.8.

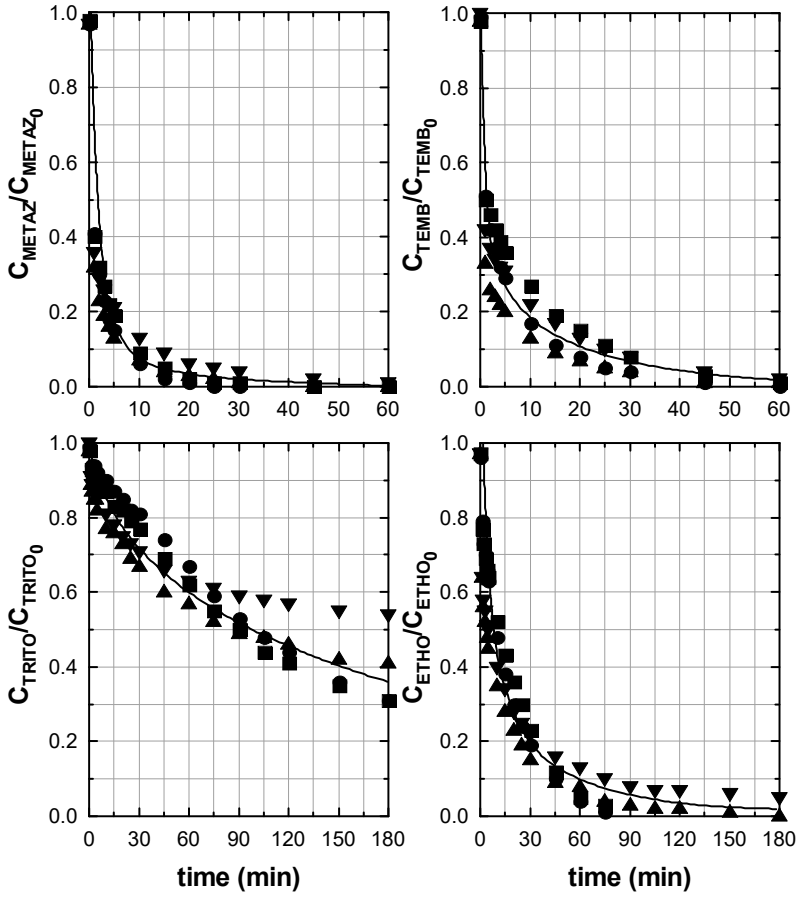

Fig. 4 Oxone® promoted photocatalytic elimination of herbicides. Catalyst load influence. Experimental conditions: $C_{Herbicide}$ = 1.0 mg L^{-1} each, pH = 7.0, T = 15-20°C, Ratio Co/Ti= 0.1:1, $C_{Oxone®}$ = 1.5 10^{-4} M, C_{CAT} (g L^{-1}): ●, 0.05; ■, 0.10; ▲, 0.25; ▼, 0.50.

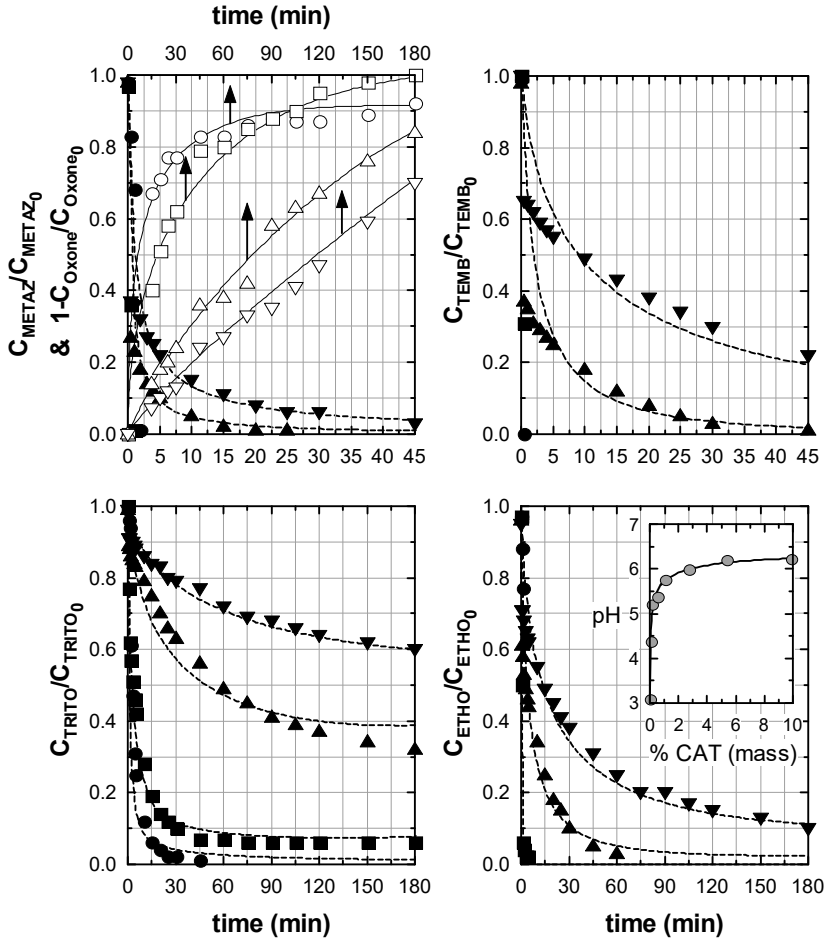

Fig. 5 Oxone® promoted photocatalytic elimination of herbicides. pH influence. Experimental conditions: $C_{Herbicide}$ = 1.0 mg L^{-1} each, T = 15-20°C, Ratio Co/Ti= 0.1:1, $C_{Oxone®}$ = 1.5 10^{-4} M, C_{CAT} = 0.5 g L^{-1}, pH: ●, 5; ■, 6; ▲, 7; ▼, 8. Open symbols correspond to Oxone® conversion. Dashed lines: Theoretical calculations with n = 0.5-0.8. Inlet bottom-right figure: pH_{pzc} determination

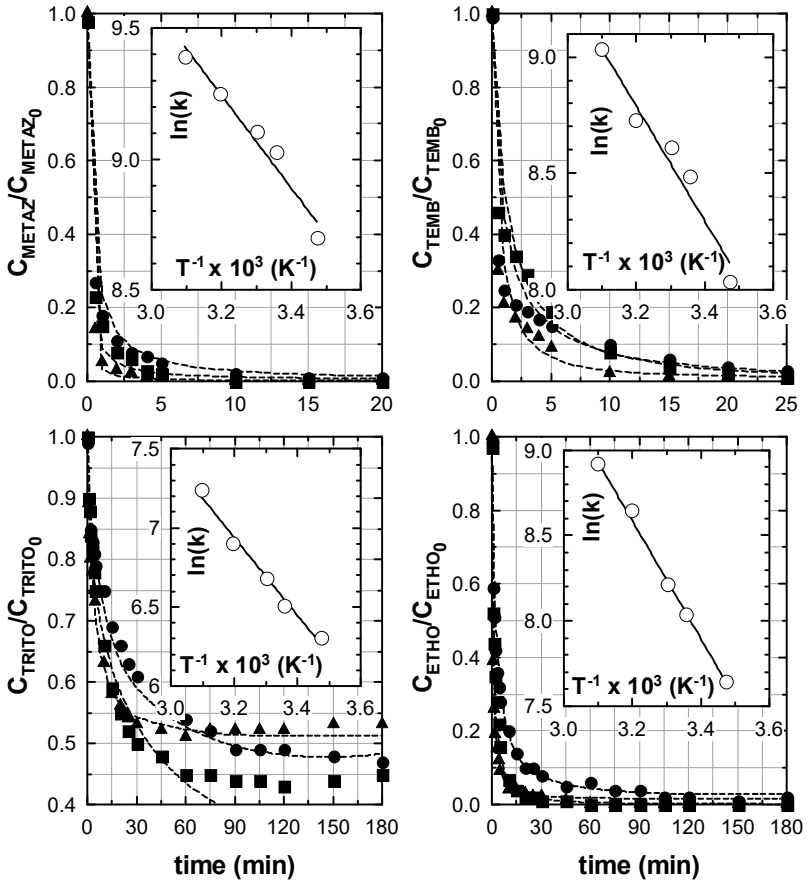

Fig. 6 Oxone® promoted photocatalytic elimination of herbicides. Temperature influence. Experimental conditions: $C_{Herbicide}$ = 1.0 mg L^{-1} each, pH = 7, Ratio Co/Ti= 0.1:1, $C_{Oxone®}$ = 1.0 10^4 M, C_{CAT} = 0.5 g L^{-1}, T (°C): ●, 30; ■, 40; ▲, 50. Inset figures correspond to Arrhenius plot. Dashed lines: Theoretical calculations with n = 0.5-0.8.

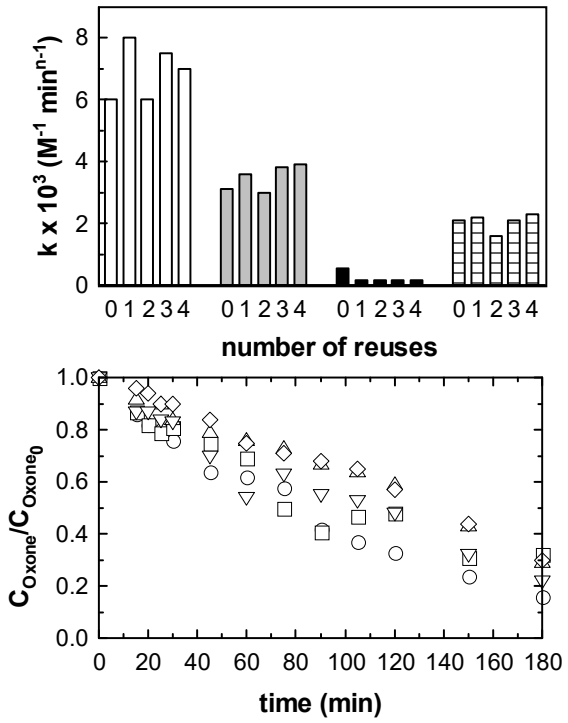

Fig. 7 Oxone® promoted photocatalytic elimination of herbicides. Catalyst stability. Experimental conditions: $C_{Herbicide}$ = 1.0 mg L^{-1} each, pH = 7, Ratio Co/Ti= 0.1:1, $C_{Oxone®}$ = 1.5 10^4 M, C_{CAT} = 0.5 g L^{-1}, T = 20 ºC. Top figure, calculated k value with n = 0.8 (metazachlor) and n=0.5 (rest) according to equation 10: white bars, metazachlor; grey bars, tembotrione; black bars, tritosulfuron; striped bars, ethofumesate. Bottom figure oxone® decomposition, number of reuses: ○, initial; □, 1st reuse; Δ, 2nd reuse; ∇, 3rd reuse; ◊, 4th reuse

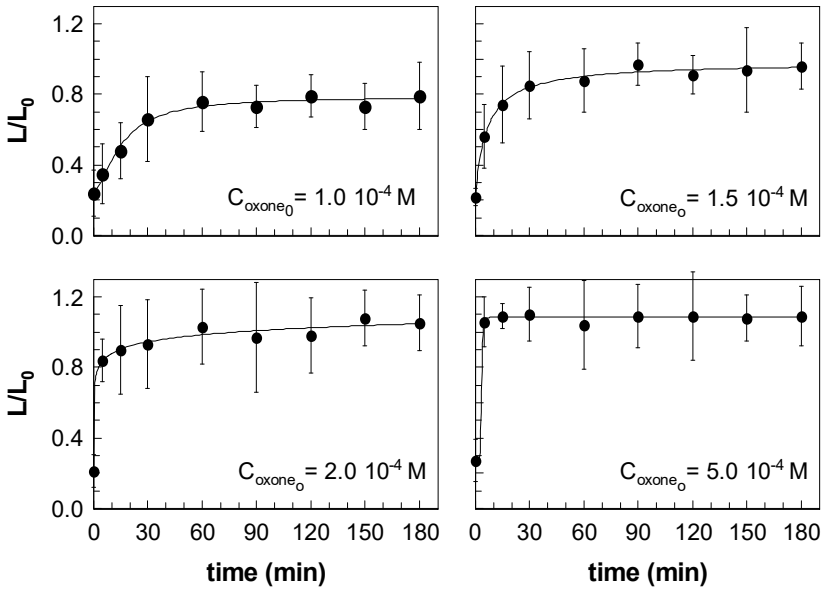

Fig. 8 Oxone® promoted photocatalytic elimination of herbicides. Phytotoxicity evolution. Experimental conditions: $C_{Herbicide}$ = 1.0 mg L^{-1} each, pH = 7, Ratio Co/Ti= 0.1:1, C_{CAT} = 0.5 g L^{-1}, T = 20 ºC. Variation of phytotoxicity (expressed as normalized root length) during treatment time at different Oxone® concentration.

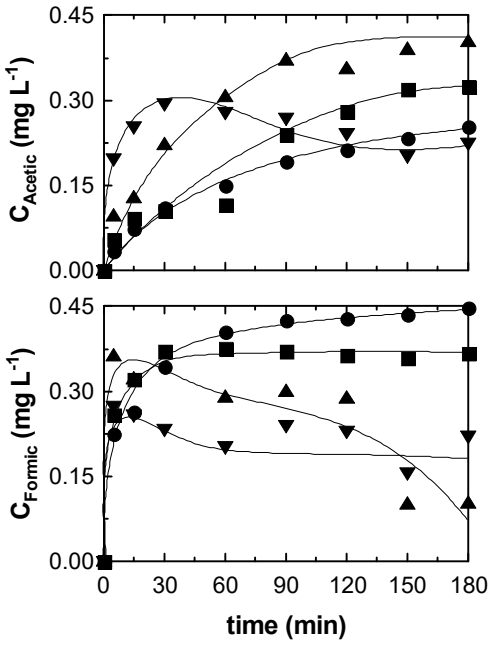

Fig. 9 Oxone® promoted photocatalytic elimination of herbicides. Evolution of released acetic and formic acids. Experimental conditions: $C_{Herbicide}$ = 1.0 mg L^{-1} each, T = 15-20 ºC, Ratio Co/Ti= 0.1:1, C_{CAT} = 0.5 g L^{-1}, pH=7, $C_{Oxone®}\cdot 10^4$ (M): ●, 1.0; ■, 1.5; ▲, 2.0; ▼, 5.0.

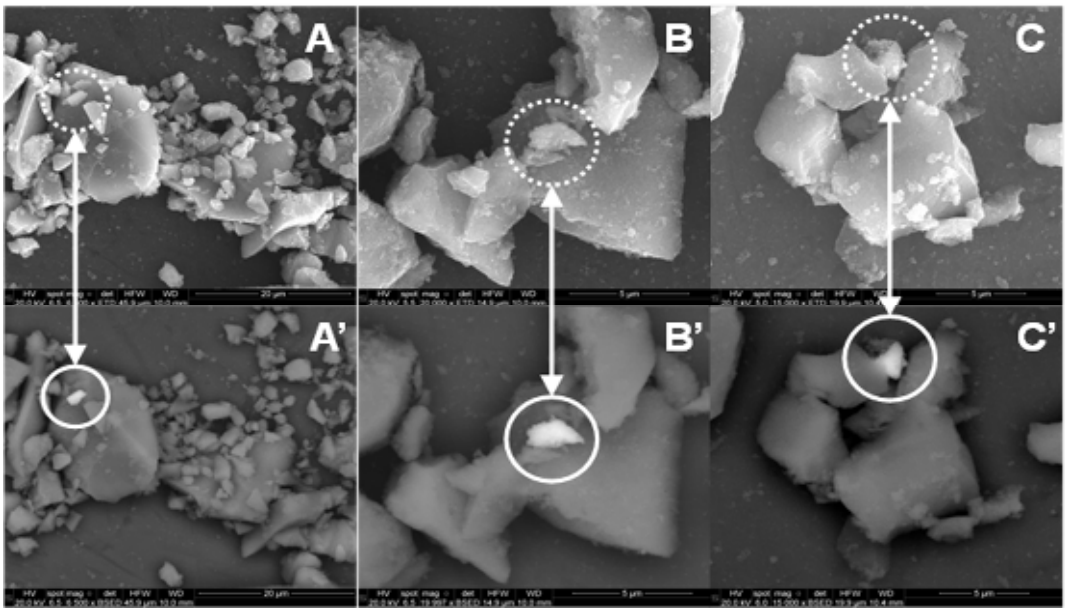

Fig. 10 SEM images of $LaCoO_3$-TiO_2 (Co/Ti=0.1:1) obtained from secondary electron (A, B and C) and their corresponding's from backscattered electron (A', B' and C')

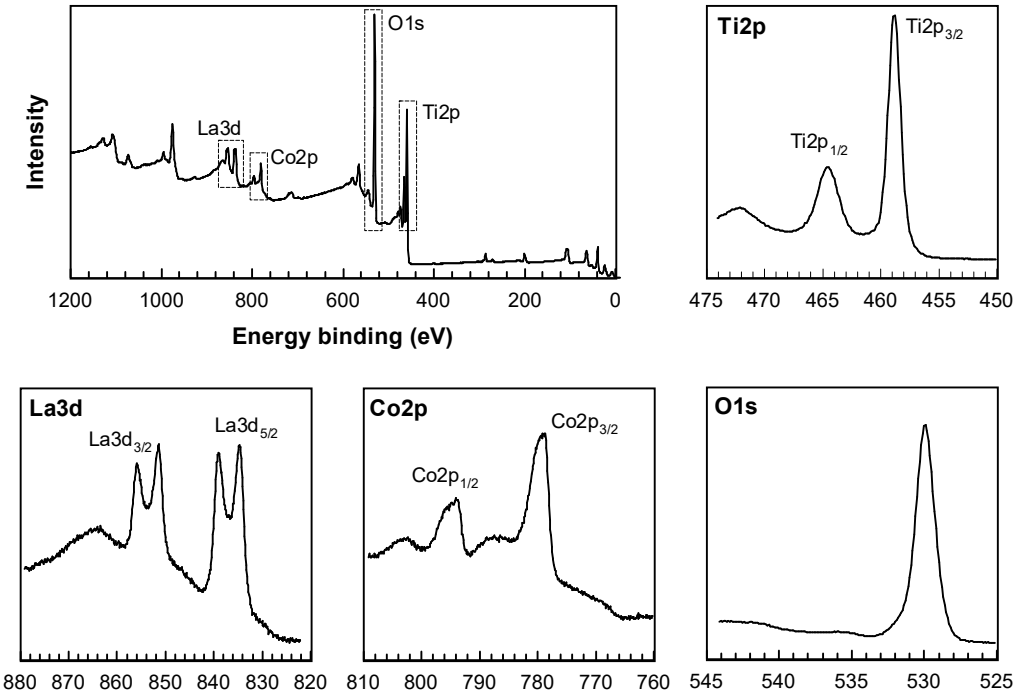

1

2 **Fig. 11** XPS spectra of $LaCoO_3$-TiO_2 (Co/Ti=0.1:1)

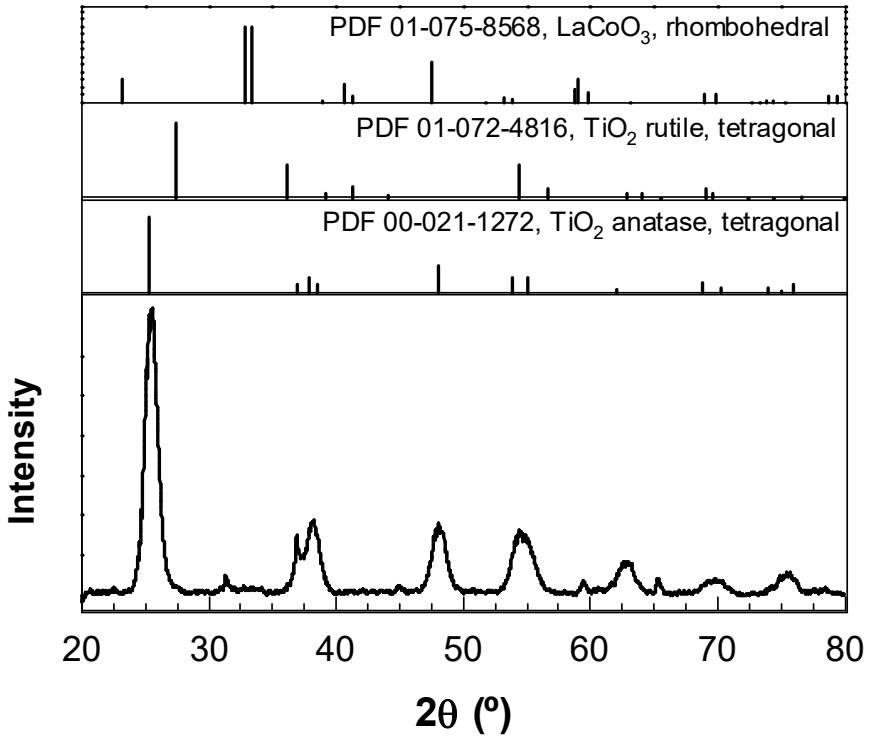

1

2 **Fig. 12** XRD diffractogram of $LaCoO_3$-TiO_2 (Co/Ti=0.1:1)

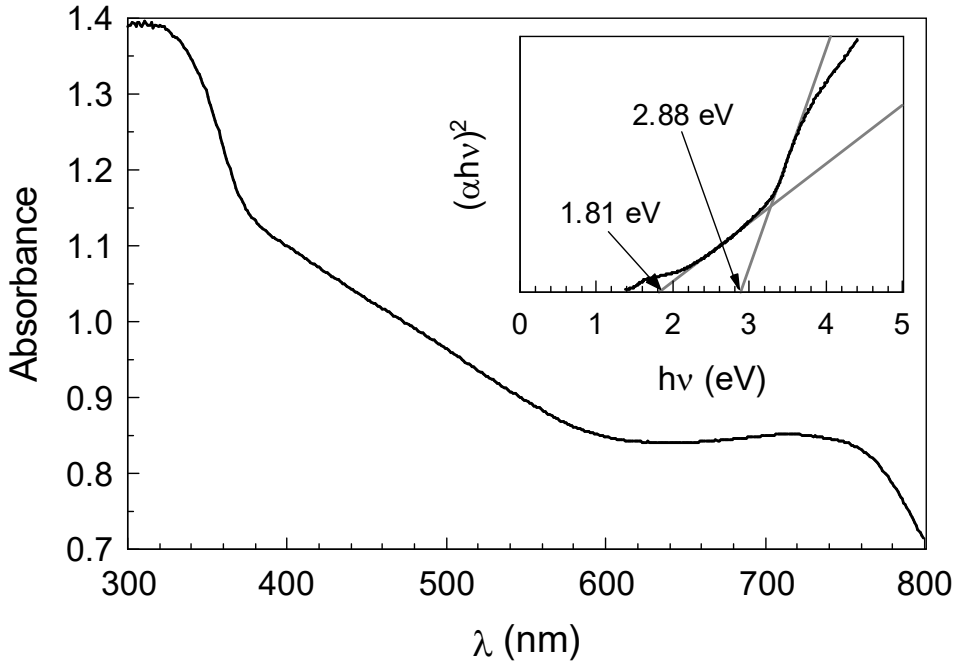

Fig. 13 Diffuse reflectance UV-vis spectra of $LaCoO_3$-TiO_2 (Co:Ti=0.1:1). Inset figure: Tauc's plot for bandgap determination